



HAL
open science

Memory Re-Condensation

Nicolas Lavielle, Daniel Beysens, Anne Mongruel

► **To cite this version:**

Nicolas Lavielle, Daniel Beysens, Anne Mongruel. Memory Re-Condensation. *Langmuir*, 2023, 39 (5), pp.2008-2014. 10.1021/acs.langmuir.2c03070 . hal-04005182

HAL Id: hal-04005182

<https://hal.science/hal-04005182>

Submitted on 6 Mar 2023

HAL is a multi-disciplinary open access archive for the deposit and dissemination of scientific research documents, whether they are published or not. The documents may come from teaching and research institutions in France or abroad, or from public or private research centers.

L'archive ouverte pluridisciplinaire **HAL**, est destinée au dépôt et à la diffusion de documents scientifiques de niveau recherche, publiés ou non, émanant des établissements d'enseignement et de recherche français ou étrangers, des laboratoires publics ou privés.

Memory re-condensation

Nicolas Lavielle*, Daniel Beysens and Anne Mongruel

Physique et Mécanique des Milieux Hétérogènes, CNRS, ESPCI, PSL Research University,
Sorbonne Université, Sorbonne Paris Cité, 75005 Paris, France

Corresponding author: nicolas.lavielle@espci.fr

Abstract:

This paper reveals a phenomenon of memory in dropwise condensation in open air. After a first condensation process and complete evaporation of the condensed droplets, further condensations proceed with droplet nucleating at the very places where former droplets evaporated. The origin of this phenomenon is due to the incorporation of airborne salts during the first droplet condensation and its further concentration during droplet evaporation. Salts act as preferential nucleation sites and humidity sinks. The potential impact of this phenomenon on controlled breath figure patterns and plants metabolism is discussed.

Keywords: Heterogeneous nucleation, condensation, breath figure, dew pattern, plant nutrition

Introduction:

Condensation is used in various industrial applications, such as heat transfer^{1,2}, desalination³, power generation⁴ or water harvesting^{5,6}. In nature, dew water is a source of fresh water for vegetation⁷⁻⁹ and consequently for wildlife. Water vapour condensation occurs on a surface when its temperature is below the dew point temperature of the surrounding humid air. In the case of dropwise condensation, droplets are formed in a partial wetting state leading to a pattern of droplets called “breath figure” (BF)^{10,11}. Heterogeneous nucleation preferentially takes place on surface defects where molecules aggregate and forms a liquid cluster. Then, the droplets grow by the direct accretion of pure water molecules through a diffusive boundary layer. Coalescences upon contact with neighbouring drops speed up the growth process¹². When the temperature of the surface becomes larger than the dew point temperature, condensation stops and water evaporates. This cycle is present in nature. At night, the air temperature decreases and its relative humidity increases, which are propitious conditions for dew condensation. In the morning, when the sun rises, the air temperature increases and relative humidity decreases, which leads to the evaporation of the condensed dew droplets.

Heterogeneous nucleation is known to take place on surface defects. The control of the nucleation sites and subsequent localization of the droplets is thus difficult to achieve. Patterned surfaces for controlled nucleation have been successfully engineered by considering that heterogeneous nucleation is favoured on hydrophilic surfaces¹³⁻¹⁵, soft surfaces^{16,17} or chemical defects¹⁸. Another approach consists in the deposition of a NaCl saturated water droplet or NaCl crystals on a surface prior condensation. It was shown that

water preferentially condenses on the salty droplet surrounding by a region of inhibited condensation¹⁸. The same observation was made by using hygroscopic droplets¹⁹.

Here, we propose to investigate another process, herein referred to as the "memory re-condensation". After complete evaporation of a first breath figure, and in the absence of any controlled nucleation sites, the new condensed pattern is expected to be totally independent of the former evaporated figure. However, and remarkably, we observe that droplets preferentially condense at the very place where the former droplets were located. This suggests that preferential nucleation sites have been created in relation to the evaporation of the former BF. Surprisingly, this phenomenon has not been studied so far, although indirectly evidenced by Yu et al²⁰. The potential impacts for plants metabolism and controlled BF patterns are also discussed.

Results and discussion:

Breath figure patterns of re-nucleation

Water condensation was performed on a model surface (silicon wafer) in a mini-climatic chamber equipped with an optical microscope. Condensation was performed for a given time until a first BF of droplets was obtained. Then, the surface was placed outside the chamber to induce a complete and natural evaporation of the water droplets under ambient conditions. Upon total disappearance of the droplets, as verified with microscope, the surface was replaced in the climatic chamber for re-condensation and observed under microscope.

Figure 1abc reports images of different BF obtained after 100, 200 and 300 s of a first condensation on a fresh silicon wafer. The nucleation of droplets preferentially occurs on the surface defects. As time proceeds, droplets grow by direct accretion of water vapour and by coalescences. The smaller droplets in (c) originate from a re-nucleation process in the free space left by coalescence events at large times. They come from the natural evolution of the BF pattern¹¹. The lower images (d,e,f) correspond to the initial BF of a second condensation on the surfaces (a,b,c) respectively, after complete evaporation of the former BFs. Note that the patterns (d,e,f) are concerned with the first moments of the second condensation, when the drops are still small and are therefore situated where they have nucleated. At large times, the position of nucleation sites becomes progressively lost because of coalescences. One can observe that the BFs obtained in the first moments of re-condensation in Figure 1(def) seem to follow a specific pattern with well-defined inter-drops characteristic size. Remarkably, the characteristic inter-drop distance is larger when the duration of the first condensation is larger. To quantify this effect, the average distance between the closest neighbour major droplets ($\langle d \rangle$) was measured and displayed on images of Figure 1, and the correlation between $\langle d_{\text{cond.}} \rangle$ and $\langle d_{\text{re-cond.}} \rangle$ is reported in Figure S1. The results indicate that the first BF pattern of condensed droplets seems to play a crucial role on the early pattern obtained from re-condensation. For comparison, Figure 2a presents the firstly condensed droplets from a surface washed from condensation history and displays no specific pattern.

To test the robustness of this phenomenon, a set of four experiments was performed. Four given BF obtained from a first condensation, similar to the BF in Figure 1b, were (a) washed under water and dried with compressed air gun, (b) left for natural evaporation in ambient conditions, (c) dried with compressed air gun and (d) left for natural evaporation in ambient conditions and further dried with compressed air gun, respectively. The images of second condensation on these surfaces are displayed in Figure 2. Experiments (a) and (c) give a BF showing no special repartition of nucleation sites (Figures 2a and 2c). By contrast, Figure 2b and Figure 2d, presenting the results obtained from experiments (b) and (d) show the same characteristic nucleation pattern, with preferential nucleation sites. This set of experiments thus evidences the key role of natural droplet evaporation on the surfaces and the robustness of the phenomenon under air flow. However, washing with water or direct gun drying cancels memory re-nucleation.

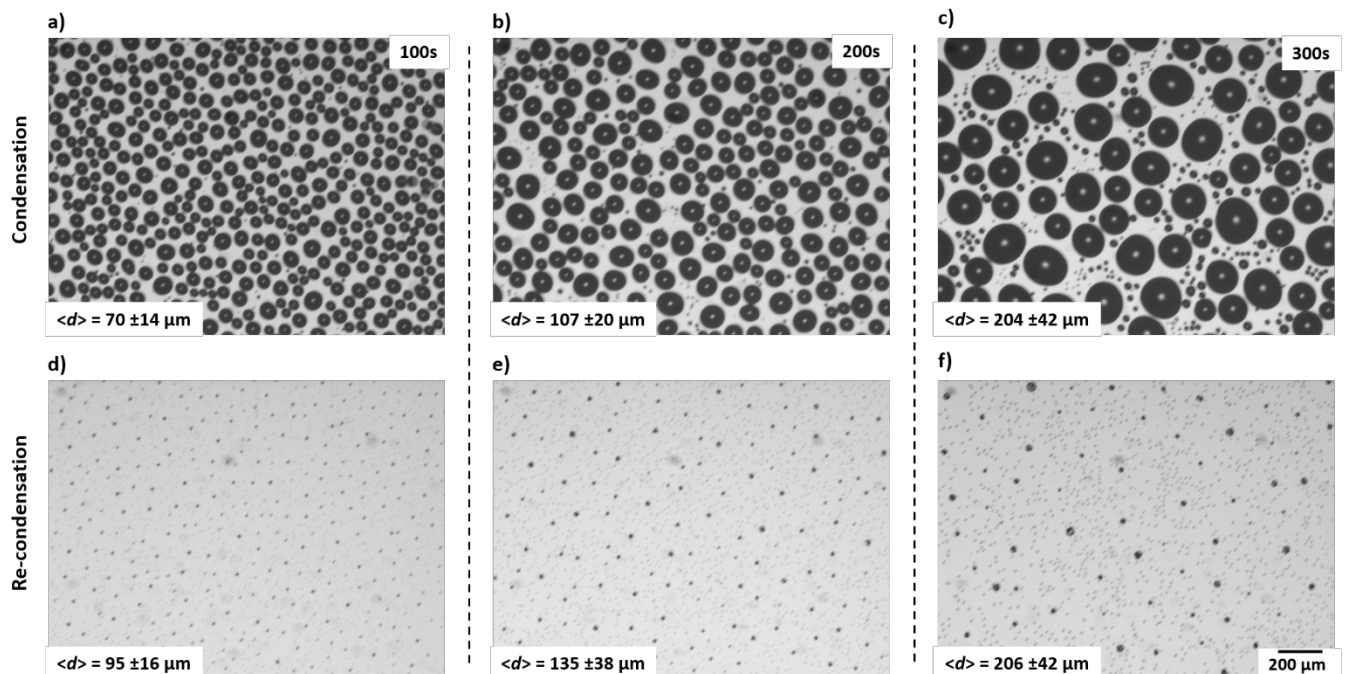


Figure 1: Re-nucleation patterns: Microscope pictures of different BFs obtained after (a) 100, (b) 200 and (c) 300 s of water vapour first condensation. The BFs were then left for natural evaporation under ambient conditions until complete disappearance. The re-nucleation pattern obtained from the former BFs (a, b, c) are shown in (d, e, f) respectively. The distance $\langle d \rangle$ is the average distance between the closest neighbour major droplets. (The scale bar applies to all images).

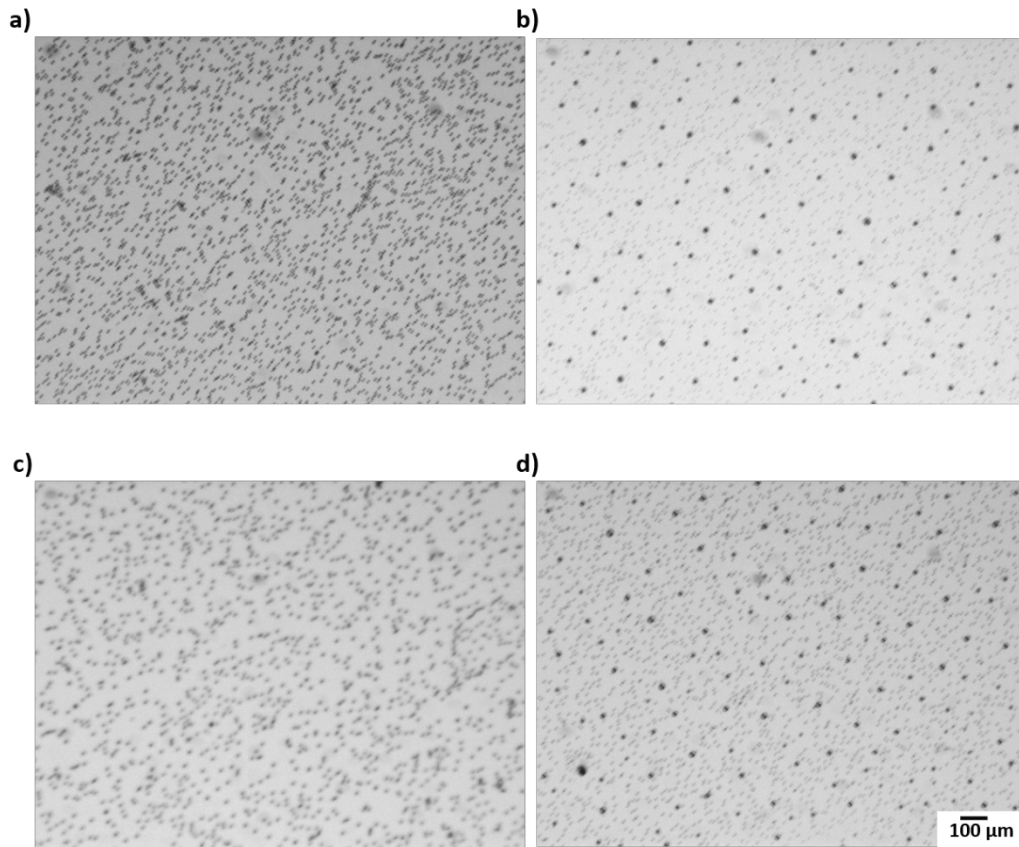


Figure 2: Experimental conditions for memory re-condensation: Optical microscope images of the re-nucleation pattern obtained on a surface after a first condensation BF (obtained after 200s of condensation) submitted to: (a) washing under water and drying with compressed air gun, (b) natural evaporation in ambient conditions, (c) drying with compressed air gun and (d) natural evaporation in ambient conditions and further drying with compressed air gun.

Localisation of re-nucleation sites

In order to establish precisely the relationship between BFs from the first and second condensation, a cycle of first condensation, evaporation and second condensation was performed on a surface placed inside the mini-climatic chamber during the whole process. Continuous observation under the microscope allowed to precisely identify the localization of the droplets. Figure 3a is an image of the droplets formed during the early stage of the second condensation. The localization of their centres is labelled by a red dot and replicated in Figure 3b and 3c. Figure 3b is the BF obtained after 100 s of the first condensation. Figure 3c is an image of the BF of Figure 3b under evaporation, just before the droplets disappear. One can observe that in the second condensation, drops nucleate at the place where the droplets from the former condensation were located. The nucleation sites of the second condensation are not situated exactly at the centre of the evaporating droplet. As evaporation proceeds, it can be observed that they are rather situated at the periphery of the droplet. This fact will be discussed below.

This experiment thus evidences the direct link between the droplets pattern from condensation and the pattern of preferential second nucleation; it confirms and explains the nucleation patterns found in Figure 1. The fact that, $\langle d_{\text{re-cond.}} \rangle$ is superior to $\langle d_{\text{cond}} \rangle$ in Figure 1a and b could indicate that larger droplets lead to a more efficient second nucleation on their localizations, compared to smaller droplets.

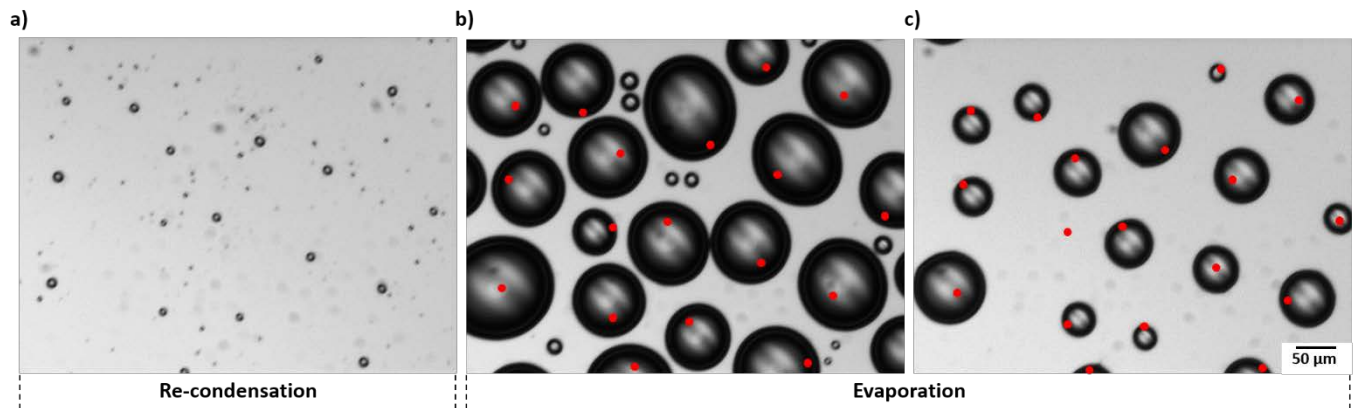


Figure 3: Localization of re-nucleation sites: (a) Optical microscopy image of the first droplets obtained from re-nucleation. The position of the centre of each major droplet is marked by a red dot and transferred to images (b) and (c). (b) Original BF after 100 s of condensation. Evaporation starts after that time. (c) BF of (b), just before complete droplets evaporation.

In order to further investigate the origin of memory condensation, a 1 μL droplet of di-ionized (DI) water was deposited on a silicon wafer and left for natural evaporation under ambient conditions. Figure 4a presents the evolution of the evaporation of the water droplet. At 1340 s, the droplet is almost completely evaporated. After a few more seconds, no water is present on the surface. Nevertheless, a persistent dark "stain" is observed later at 2000 s at the place of the evaporated droplet. As one will see later, the deposition of the stain from the water droplet is at the origin of the memory re-condensation phenomenon. Figure 4b reports the condensation pattern obtained in the vicinity of this stain. A large droplet is seen where the stain was located, surrounded by a zone of inhibited condensation. This pattern is characteristic of a droplet pattern around a humidity sink¹⁸.

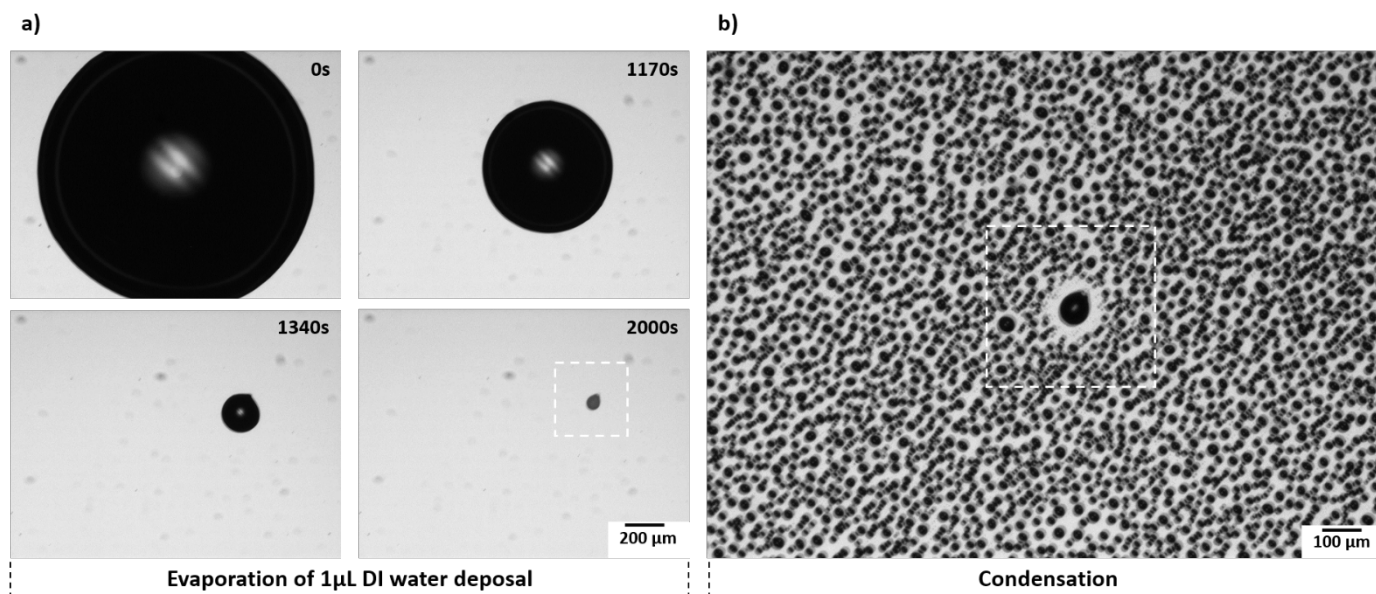


Figure 4: Condensation pattern on silicon wafer after the evaporation of a water droplet: (a) Optical microscopy images of the time evolution of the evaporation of 1 μL ultrapure deionized water droplet on silicon wafer evidencing the deposition of a persistent stain after complete droplet evaporation (middle of the interrupted white square). (b) BF of condensation around the stain (middle of the interrupted white square), which acts as a site of preferential condensation or humidity sink with a region of inhibited condensation.

Origin of memory re-condensation

The stain left by the evaporation of water droplets on model silicon wafer surfaces was characterized by scanning electron microscope (SEM) to image the surface morphology and energy dispersive X-ray spectroscopy (EDX) to identify and quantify the chemical elements. The study was carried out on two different stains for comparison: the first stain was obtained after the evaporation of water droplets deposited outdoor by natural dew, the second stain resulted from the evaporation of a 1 μL DI water droplet deposition. Outdoor dew water was harvested on a silicon wafer on the terrace of the laboratory located in Paris downtown. The dew droplets naturally evaporated upon sunrise. The sample was then analysed under SEM coupled with EDX. Figure 5 shows an electron microscope image of a typical stain left by the evaporation of dew water on the silicon surface and an EDX mapping of the chemical elements present on this image with a quantification in atomic percentage. One can observe a circular dark stain in the centre of the image with the presence of crystals inside. The chemical analysis reveals that the main detected chemical elements are Si, Na, K, Cl and C. One can notice that Si is also found on the stain, which was expected because EDX detects surface chemical elements within a thickness of 100 nm. Na, K, Cl are the principal chemical elements of the observed crystals. Carbon element is found to fit the geometry of the dark region of the stain. However, the quantification of C element is not reliable using EDX as the use of the electron beam is known to deposit carbon elements; nevertheless, more carbon is present on the stain than on the neighbouring surface as revealed by the stronger red colour, which corresponds to the stain geometry. The chemical elements (other than Si) are hypothesized to come from the absorption of airborne aerosol in dew water, which are further deposited on the surface by droplets

evaporation. Upon evaporation, the droplet increases its concentration in salts until crystallization occurs. Larger droplets can adsorb more aerosols due to their higher exchange surface, which explains why $\langle d_{re-cond.} \rangle$ can be larger than $\langle d_{cond} \rangle$ in Figure 1. In order to further characterize the “stain”, a 1 μ L DI water (resistivity of 18.2 M Ω .cm, i.e. close to pure water) droplet was placed on a silicon wafer surface in the laboratory, left for evaporation, and then the surface was analysed by the same method using SEM and EDX. Figure S2 shows the corresponding EDX image. The same crystals and chemical elements are found as in Figure 5 with natural dew water collected outside. The same observations and conclusions can be given. It confirms the hypothesis of airborne aerosol ad/absorption independent from the condensation site, located indoor or outdoor. It is indeed known²¹ that water condensation in open humid air involves the dissolution of aerosols and absorption of gases. In the experiments described above, the only possible sources of dissolved materials in the absence of chemical reaction with the substrate are the airborne particles and absorbed gases. The deposition of salts on the surface by the evaporation of a BF therefore explains the phenomenon of memory re-condensation as salts are known to act as a humidity sink¹⁸ and lead to a specific pattern during re-condensation. This deposition does not occur at the centre of the evaporating droplet (Figure 3) because the evaporation process involves a random pinning of the contact line on the silicon surface defects. The centre of mass of the droplets thus move during their evaporation.

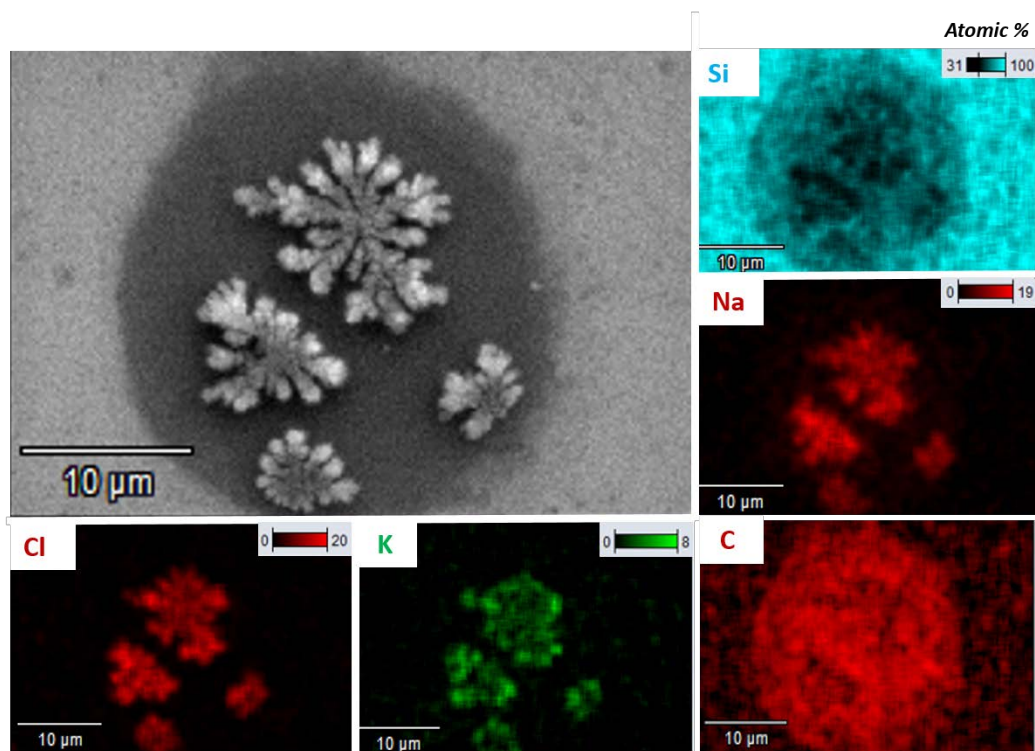


Figure 5: Origin of memory re-condensation: Scanning electron microscope (SEM) image of a typical “stain” left by the evaporation of natural dew water droplets and energy dispersive X-ray spectroscopy (EDX) mapping of the SEM image for the identification and quantification (in atomic %) of the chemical elements comprising the stain.

The above findings suggest that memory re-condensation is a phenomenon of preferential condensation observed on any surface subjected to dropwise condensation in open air, when airborne aerosols can be adsorbed at the droplet-air interface. It is characterized by a pattern of nucleated droplets at the very place where, after a first condensation, the original droplet pattern evaporated. Each droplet leaves small salt crystals on the surface, which act as a preferential nucleation site for the next condensation.

Condensation of water vapour from natural unfiltered humid air involves the absorption of gases, a fast process, and the dissolution of aerosols^{21,22}. The absorbed gases are natural or anthropogenic, such as CO₂, SO₂, NO and NO₂. The condensing droplets, by growing and sweeping the surface by coalescences, dissolve the aerosols deposited on the substrate. They also incorporate aerosols at the liquid-air interface. These aerosols are mainly salts of sea origin (e.g. NaCl, MgCl₂) or from anthropogenic sources (e.g. CaCO₃, KCl). Other particles, such as carbon diesel particles, may also be incorporated. The chemical analysis in Figures 5 and S2 shows that the main dissolved salt is NaCl, of sea origin. Paris is indeed within 200 km from the Channel and 500 km from the Atlantic Ocean and its climate is Marine West Coast Climate according to the Köppen Classification.

The stains left by evaporation of a BF are dependent on the way solubilized or particulate materials are incorporated in the droplet during condensation, and on the thermo-capillary flows and contact line de-pinning arising during droplet evaporation. This complex processes may lead to various deposition patterns²³, that will in turn impact the re-nucleation patterns. In the present case, dendrite stains such as seen in Figures 5 and S2 are generally observed after the evaporation of a BF condensed on Si wafers. During droplet evaporation, the concentration of dissolved salts increases until reaching the oversaturation of solute, thus leading to crystallization. This process is different from the drying of a droplet containing insoluble particles, leading to a ring deposition pattern^{24,25}. A precise investigation of the crystallization pattern and crystal morphology is, however, out of the scope of the present paper.

The chemical nature of the substrate materials will matter to determine the liquid-surface interactions and the values of the contact angles and contact angle hysteresis upon condensation and evaporation. In addition, a chemical reaction with condensed water and/or with the elements in the stain and the substrate may also occur depending on the materials used for the substrate. This reaction could permanently modify the geometrical and chemical properties of the substrate. In the present case, where the stains are mainly composed of Na, K, Cl and C and the substrate is silicon, protected by a surface layer of silicon dioxide, no permanent substrate modification are seen. As a matter of fact, stains can easily be washed away using water or compressed air. Also, one observes the loss of memory at large condensation times, when the drops nucleated on the stains have coalesced with other drops and have moved on the substrate.

Beyond the awareness and knowledge of the existence of the memory re-condensation phenomenon, the results presented here could have applicative impacts in industry and for the understanding of vegetation metabolism. Indeed, the patterning of BFs themselves can be of interest for the precise patterning of polymer films or materials to generate controlled templates by the BF method²⁶⁻²⁸. Potential applications are textured surfaces^{29,30}, responsive surfaces³¹, filtration³² or catalysis³³. Patterned BFs could also find applications in patterned chemistry for biomedical applications^{34,35}, in aqueous media. For the generation of a controlled BF pattern, 0.2µL water droplets were deposited on a silicon wafer surface in the

shape of a ring, then condensation was performed post complete evaporation. Figure 6 presents the original deposited “BF” and the corresponding BF of condensation post evaporation. Figure 6 exhibits an efficient controlled patterning of the condensed water droplets.

Memory re-nucleation has evidenced the deposition of salts and chemical elements from natural dew water evaporation on a surface, such as Na, Cl, K and C. These elements are adsorbed from air at the air-water interface. Chemical analysis of collected dew water in Paris revealed the presence of numerous ions in its water as well²¹. The same phenomenon should be taking place on the leaves of plants when dew forms. Dew is known as an important resource of water for plants⁹, especially in arid climates or dry soils. It is expected from the above results that dew could also be a vector of macro-nutrients for plants nutrition. Carbon is a nutrient for plants, a major constituent of organic material, involved in enzymatic processes and assimilated by oxidation-reduction reaction³⁶. K, Na and Cl are involved in enzymatic reactions, osmotic potential, membrane permeability and electrochemical potentials³⁶. K and Cl belong to the top 10 essential elements for plants growth^{36,37}. Uptake of elements from leaves can take place by penetration of the external plant surface through the cuticle or stomata³⁸. Actually, foliar sprays are widely used in agriculture and showed better efficiency than soil fertilization as nutrients are directly delivered to sink organs³⁸. We hypothesize dew to possibly be an additional and unsuspected vesicle of macro-nutrients for plants.

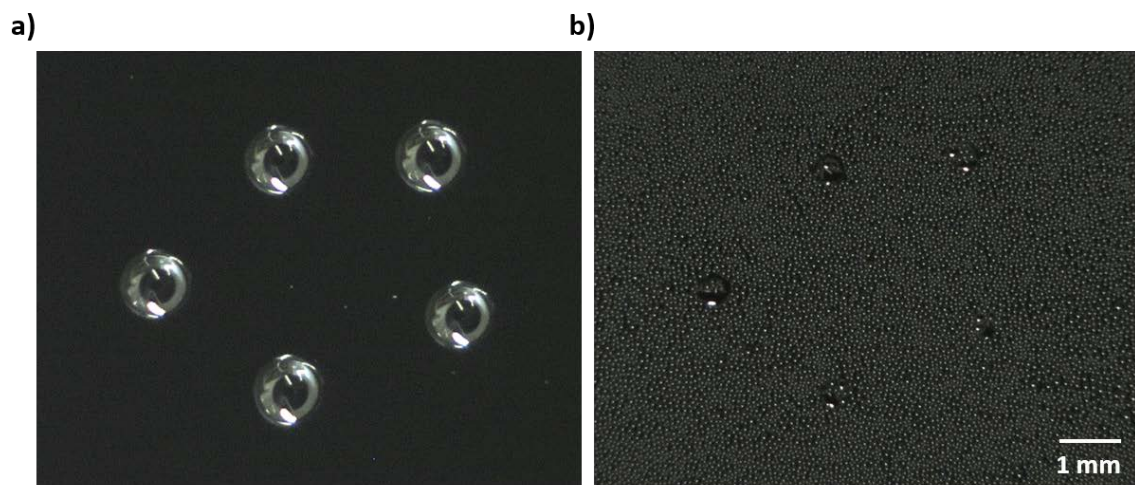


Figure 6: Controlled re-condensation pattern: (a) Deposition of 0.2µL water droplets as a ring pattern. (b) BF of condensation post complete evaporation of droplets from a).

Methods:

Condensation, DI water droplet deposal and re-nucleation under optical microscope

To generate BFs, condensation was performed for different times (100, 200 and 300s) on silicon wafers (GlobalWafers) in a home-made mini climatic chamber mounted on an optical microscope (Leica DMRXE) equipped with a camera (Imaging Source, DFK 23U445). The mini climatic chamber is composed of: A Peltier thermostat for conductive cooling, on which is placed the samples – A polystyrene cover to hermetically lock the samples with a top opening for a sealed glass slide for optical observation and two side openings for the

entrance of saturated humid air – Pump (Rena 101) and tubing are used to inject air in a bath of water in order to re-inject saturated humid air to the two side openings of the sealed mini-chamber. The relative humidity in the mini chamber is 90%. The Peltier element is submitted to a current of 2V and 0.5A (generator, Sodilec SDRI 205) and a flow of cooled water at 10°C (Heto CBN 8-30 and HMT 200) in order to always set the surface temperature of the Peltier at 4°C. The deposition of desired volume of DI water (resistivity of 18.2 MΩ.cm, the value of pure water) on silicon wafer surfaces was performed with a micropipette (VWR) to study re-nucleation after single droplet and ring patterned droplets deposals. Re-nucleation experiments were performed post complete evaporation of the condensed or deposited droplets. Evaporation took place either outside the mini-climatic chamber in ambient conditions, or inside the mini-climatic chamber (to do not lose the precise localization of evaporating droplets) by the passive increase of the surface temperature to ambient conditions, turning off the Peltier element and opening the mini-climatic chamber. To observe the first re-condensed droplets, the surface of the sample was gently cooled down below the dew point temperature of the lab, without sealing the climatic chamber and without saturated humid air injection; to enable a slow re-nucleation for visualization purpose. Surface temperature of the Peltier is monitored along the experiments using thermocouple sensors and software Picolog. ICCapture software was used for the images sequence acquisition (1 image per second). ImageJ software was used to measure the average distance between the closest neighbour major droplets ($\langle d \rangle$).

Characterization of the “stain”

To evaluate the robustness of the stain left by the evaporation of condensed or deposited water droplets, the following scenarios were studied post condensation (for 200s, under the experimental conditions described above) and before re-nucleation: (1) natural evaporation in ambient conditions or (2) washing under water and drying with compressed air gun or (3) drying with compressed air gun or (4) natural evaporation in ambient conditions and further drying with compressed air gun. Two types of stains were analysed under scanning electron microscopy (SEM) coupled to energy dispersive X-ray spectroscopy (EDX): (1) Stain left by natural dew evaporation on silicon wafer and (2) stain left by 1μL DI water deposal and evaporation on silicon wafer in laboratory. Natural dew was obtained in a morning of march when meteorological conditions were met to form dew, on the roof of the Institut de Physique du Globe de Paris; equipped with a weather station (temperature, relative humidity and wind force/direction sensors) (Davis). SEM and EDX were performed with a SEM Quattro (Thermofisher) under a voltage of 15 kV and intensity of 0.22 nA; the samples were placed 10 mm below the source of the electron beam. SEM was used to characterize the morphology of the stain. For EDX, X-ray emission spectra were integrated to identify and quantify (in atomic percentage) the present chemical elements on the studied surface and chemical mapping was generated to localize the detected elements.

Supporting information

- Experimental conditions to obtain memory re-condensation

- Morphological and chemical analysis of the stain left by the evaporation of a DI water droplet at the origin of the phenomenon of memory re-condensation.

Acknowledgements

This project received the support from the METAWATER Project (No. ANR-20-CE08-0023 META-WATER).

Conflict of Interest

The authors declare no conflict of interest.

References:

- (1) Cho, H. J.; Preston, D. J.; Zhu, Y.; Wang, E. N. Nanoengineered Materials for Liquid–Vapour Phase-Change Heat Transfer. *Nat Rev Mater* **2017**, *2* (2), 16092. <https://doi.org/10.1038/natrevmats.2016.92>.
- (2) Preston, D. J.; Lu, Z.; Song, Y.; Zhao, Y.; Wilke, K. L.; Antao, D. S.; Louis, M.; Wang, E. N. Heat Transfer Enhancement During Water and Hydrocarbon Condensation on Lubricant Infused Surfaces. *Sci Rep* **2018**, *8* (1), 540. <https://doi.org/10.1038/s41598-017-18955-x>.
- (3) Khawaji, A. D.; Kutubkhanah, I. K.; Wie, J.-M. Advances in Seawater Desalination Technologies. *Desalination* **2008**, *221* (1–3), 47–69. <https://doi.org/10.1016/j.desal.2007.01.067>.
- (4) Zhao, X.; Wu, G.; Qi, J.; to Baben, M.; Müller, M. Investigation on the Condensation Behavior of the Trace Element Zinc in (Ar/H₂O/HCl/H₂S) Gas Mixtures and Its Practical Implications in Gasification-Based Processes for Energy and Power Generation. *Fuel* **2021**, *295*, 120600. <https://doi.org/10.1016/j.fuel.2021.120600>.
- (5) Lee, A.; Moon, M.-W.; Lim, H.; Kim, W.-D.; Kim, H.-Y. Water Harvest via Dewing. *Langmuir* **2012**, *28* (27), 10183–10191. <https://doi.org/10.1021/la3013987>.
- (6) Liu, X.; Beysens, D.; Bourouina, T. Water Harvesting from Air: Current Passive Approaches and Outlook. *ACS Materials Lett.* **2022**, *4* (5), 1003–1024. <https://doi.org/10.1021/acsmaterialslett.1c00850>.
- (7) D. Makowski, R. M. Effect of Inoculum Concentration, Temperature, Dew Period, and Plant Growth Stage on Disease of Round-Leaved Mallow and Velvetleaf by *Colletotrichum Gloeosporioides* f. Sp. *Malvae*. *Phytopathology* **1993**, *83* (11), 1229. <https://doi.org/10.1094/Phyto-83-1229>.
- (8) Hill, A. J.; Dawson, T. E.; Shelef, O.; Rachmilevitch, S. The Role of Dew in Negev Desert Plants. *Oecologia* **2015**, *178* (2), 317–327. <https://doi.org/10.1007/s00442-015-3287-5>.
- (9) Munné-Bosch, S.; Alegre, L. Role of Dew on the Recovery of Water-Stressed Melissa Officinalis L. Plants. *Journal of Plant Physiology* **1999**, *154* (5–6), 759–766. [https://doi.org/10.1016/S0176-1617\(99\)80255-7](https://doi.org/10.1016/S0176-1617(99)80255-7).
- (10) Baker, T. J. LXV. *Breath Figures*. *The London, Edinburgh, and Dublin Philosophical Magazine and Journal of Science* **1922**, *44* (262), 752–765. <https://doi.org/10.1080/14786441108634040>.
- (11) Beysens, D.; Knobler, C. M. Growth of Breath Figures. *Phys. Rev. Lett.* **1986**, *57* (12), 1433–1436. <https://doi.org/10.1103/PhysRevLett.57.1433>.

- (12) Beysens, D. Dew Nucleation and Growth. *Comptes Rendus Physique* **2006**, *7* (9–10), 1082–1100. <https://doi.org/10.1016/j.crhy.2006.10.020>.
- (13) Hou, Y.; Yu, M.; Chen, X.; Wang, Z.; Yao, S. Recurrent Filmwise and Dropwise Condensation on a Beetle Mimetic Surface. *ACS Nano* **2015**, *9* (1), 71–81. <https://doi.org/10.1021/nn505716b>.
- (14) Bai, H.; Wang, L.; Ju, J.; Sun, R.; Zheng, Y.; Jiang, L. Efficient Water Collection on Integrative Bioinspired Surfaces with Star-Shaped Wettability Patterns. *Adv. Mater.* **2014**, *26* (29), 5025–5030. <https://doi.org/10.1002/adma.201400262>.
- (15) Dai, X.; Sun, N.; Nielsen, S. O.; Stogin, B. B.; Wang, J.; Yang, S.; Wong, T.-S. Hydrophilic Directional Slippery Rough Surfaces for Water Harvesting. *Sci. Adv.* **2018**, *4* (3), eaaq0919. <https://doi.org/10.1126/sciadv.aaq0919>.
- (16) Eslami, F.; Elliott, J. A. W. Thermodynamic Investigation of the Barrier for Heterogeneous Nucleation on a Fluid Surface in Comparison with a Rigid Surface. *J. Phys. Chem. B* **2011**, *115* (36), 10646–10653. <https://doi.org/10.1021/jp202018e>.
- (17) Sokuler, M.; Auernhammer, G. K.; Roth, M.; Liu, C.; Bonaccorso, E.; Butt, H.-J. The Softer the Better: Fast Condensation on Soft Surfaces. *Langmuir* **2010**, *26* (3), 1544–1547. <https://doi.org/10.1021/la903996j>.
- (18) Guadarrama-Cetina, J.; Narhe, R. D.; Beysens, D. A.; González-Viñas, W. Droplet Pattern and Condensation Gradient around a Humidity Sink. *Phys. Rev. E* **2014**, *89* (1), 012402. <https://doi.org/10.1103/PhysRevE.89.012402>.
- (19) Nath, S.; Bisbano, C. E.; Yue, P.; Boreyko, J. B. Duelling Dry Zones around Hygroscopic Droplets. *J. Fluid Mech.* **2018**, *853*, 601–620. <https://doi.org/10.1017/jfm.2018.579>.
- (20) Yu, X.; Dorao, C. A.; Fernandino, M. Droplet Evaporation during Dropwise Condensation Due to Deposited Volatile Organic Compounds. *AIP Advances* **2021**, *11* (8), 085202. <https://doi.org/10.1063/5.0056005>.
- (21) Beysens, D.; Mongruel, A.; Acker, K. Urban Dew and Rain in Paris, France: Occurrence and Physico-Chemical Characteristics. *Atmospheric Research* **2017**, *189*, 152–161. <https://doi.org/10.1016/j.atmosres.2017.01.013>.
- (22) Beysens, D. *Dew Water*; River Publishers: Gistrup, Aalborg, Denmark, 2018.
- (23) Zang, D.; Tarafdar, S.; Tarasevich, Y. Yu.; Dutta Choudhury, M.; Dutta, T. Evaporation of a Droplet: From Physics to Applications. *Physics Reports* **2019**, *804*, 1–56. <https://doi.org/10.1016/j.physrep.2019.01.008>.
- (24) Hu, H.; Larson, R. G. Evaporation of a Sessile Droplet on a Substrate. *J. Phys. Chem. B* **2002**, *106* (6), 1334–1344. <https://doi.org/10.1021/jp0118322>.
- (25) Hu, H.; Larson, R. G. Marangoni Effect Reverses Coffee-Ring Depositions. *J. Phys. Chem. B* **2006**, *110* (14), 7090–7094. <https://doi.org/10.1021/jp0609232>.
- (26) Muñoz-Bonilla, A.; Fernández-García, M.; Rodríguez-Hernández, J. Towards Hierarchically Ordered Functional Porous Polymeric Surfaces Prepared by the Breath Figures Approach. *Progress in Polymer Science* **2014**, *39* (3), 510–554. <https://doi.org/10.1016/j.progpolymsci.2013.08.006>.
- (27) Wan, L.-S.; Zhu, L.-W.; Ou, Y.; Xu, Z.-K. Multiple Interfaces in Self-Assembled Breath Figures. *Chem. Commun.* **2014**, *50* (31), 4024–4039. <https://doi.org/10.1039/C3CC49826C>.
- (28) Zhang, A.; Bai, H.; Li, L. Breath Figure: A Nature-Inspired Preparation Method for Ordered Porous Films. *Chem. Rev.* **2015**, *115* (18), 9801–9868. <https://doi.org/10.1021/acs.chemrev.5b00069>.
- (29) Zhang, P.; Chen, H.; Zhang, L.; Ran, T.; Zhang, D. Transparent Self-Cleaning Lubricant-Infused Surfaces Made with Large-Area Breath Figure Patterns. *Applied Surface Science* **2015**, *355*, 1083–1090. <https://doi.org/10.1016/j.apsusc.2015.07.159>.
- (30) Li, Z.; Ma, X.; Kong, Q.; Zang, D.; Guan, X.; Ren, X. Static and Dynamic Hydrophobic Properties of Honeycomb Structured Films via Breath Figure Method. *J. Phys. Chem. C* **2016**, *120* (33), 18659–18664. <https://doi.org/10.1021/acs.jpcc.6b06186>.
- (31) De León, A. S.; Molina, M.; Wedepohl, S.; Muñoz-Bonilla, A.; Rodríguez-Hernández, J.; Calderón, M. Immobilization of Stimuli-Responsive Nanogels onto Honeycomb Porous Surfaces and

Controlled Release of Proteins. *Langmuir* **2016**, *32* (7), 1854–1862.
<https://doi.org/10.1021/acs.langmuir.5b04166>.

- (32) Yuan, H.; Yu, B.; Cong, H.; Peng, Q.; Yang, Z.; Luo, Y.; Chi, M. Preparation of Highly Permeable BPPO Microfiltration Membrane with Binary Porous Structures on a Colloidal Crystal Substrate by the Breath Figure Method. *Journal of Colloid and Interface Science* **2016**, *461*, 232–238. <https://doi.org/10.1016/j.jcis.2015.09.019>.
- (33) Wan, L.-S.; Li, Q.-L.; Chen, P.-C.; Xu, Z.-K. Patterned Biocatalytic Films via One-Step Self-Assembly. *Chem. Commun.* **2012**, *48* (37), 4417. <https://doi.org/10.1039/c2cc17451k>.
- (34) Healy, K. Kinetics of Bone Cell Organization and Mineralization on Materials with Patterned Surface Chemistry. *Biomaterials* **1996**, *17* (2), 195–208. [https://doi.org/10.1016/0142-9612\(96\)85764-4](https://doi.org/10.1016/0142-9612(96)85764-4).
- (35) Huang, T. H.; Pei, Y.; Zhang, D.; Li, Y.; Kilian, K. A. Patterned Porous Silicon Photonic Crystals with Modular Surface Chemistry for Spatial Control of Neural Stem Cell Differentiation. *Nanoscale* **2016**, *8* (21), 10891–10895. <https://doi.org/10.1039/C5NR08327C>.
- (36) Kirkby, E. Introduction, Definition and Classification of Nutrients. In *Marschner's Mineral Nutrition of Higher Plants*; Elsevier, 2012; pp 3–5. <https://doi.org/10.1016/B978-0-12-384905-2.00001-7>.
- (37) Manning, D. A. C. Mineral Sources of Potassium for Plant Nutrition. A Review. *Agron. Sustain. Dev.* **2010**, *30* (2), 281–294. <https://doi.org/10.1051/agro/2009023>.
- (38) Eichert, T.; Fernández, V. Uptake and Release of Elements by Leaves and Other Aerial Plant Parts. In *Marschner's Mineral Nutrition of Higher Plants*; Elsevier, 2012; pp 71–84. <https://doi.org/10.1016/B978-0-12-384905-2.00004-2>.

TOC

